# An investigation into the mechanisms controlling seasonal speed-up events at a High Arctic glacier

Robert G. Bingham[1], Alun L. Hubbard[2,3], Peter W. Nienow[3] and Martin J. Sharp[4]

[1] British Antarctic Survey, Natural Environment Research Council, High Cross, Madingley Road, Cambridge, CB3 0ET, UK. Email: rgbi@bas.ac.uk

[2] Centre for Glaciology, Department of Geography and Earth Sciences, University of Wales Aberystwyth, SY23 3DB, UK.

[3] School of GeoSciences, University of Edinburgh, Drummond Street, Edinburgh, EH8 9XP, UK.

[4] Department of Earth and Atmospheric Sciences, University of Alberta, Edmonton, Alberta, T6G 2E3, Canada.

## ABSTRACT

Seasonal variations in ice motion have been observed at several polythermal ice masses across the High Arctic, including the Greenland Ice Sheet. However, such variations in ice motion and their possible driving mechanisms are rarely incorporated in models of the response of High Arctic ice masses to predicted climate warming. Here we use a three-dimensional finite-difference flow model, constrained by field data, to investigate seasonal variations in the distribution of basal sliding at polythermal John Evans Glacier, Ellesmere Island, Canada. Our results suggest that speedups observed at the surface during the melt season result directly from changes in rates of basal motion. They also suggest that stress-gradient coupling is ineffective at transmitting basal motion anomalies to the upper part of the glacier, in contrast with findings from an earlier flow-line study at the same glacier. We suggest that stress-gradient coupling is limited through the effect of high drag imposed by a partially frozen bed, and friction induced by valley walls and significant topographic pinning points. Our findings imply that stress-gradient coupling may play a limited role in transmitting supraglacially-forced basal motion anomalies through Arctic valley and outlet glaciers with complex topographic settings; and highlight the importance of dynamically incorporating basal motion into models predicting the response of the Arctic's land ice to climate change.

## INTRODUCTION

Intra-annual variations in ice motion, with higher velocities during the melt season, have been observed at several predominantly cold polythermal glaciers [*Bingham et al.*, 2003; *Müller and Iken*, 1973; *Rabus and Echelmeyer*, 1997; *Rippin et al.*, 2005] including the Greenland Ice Sheet [*Zwally et al.*, 2002]. Such seasonal speedups have typically been attributed to 'supraglacial hydraulic forcing,' the effect of supraglacial meltwater penetrating to the glacier bed and generating excess basal water pressures (or reduced basal friction) and enhanced basal motion [*Bingham et al.*, 2005; *Zwally et al.*, 2002]. These processes offer significant potential to accelerate the response of ice masses to climate warming by facilitating the rapid transmission of increasing volumes of surface runoff to the subglacial hydraulic system, thereby potentially increasing basal motion and raising the overall rate of ice flux to lower elevations [*Parizek and Alley*, 2004; *Rignot and Kanagaratnam*, 2006]. The concern is particularly acute over the High Arctic (>75°N), where substantial warming and corresponding increases in surface melting have been observed over the last two decades [*Abdalati and Steffen*, 2001; *Hanna et al.*, 2005; *IPCC*, 2007; *Steffen et al.*, 2004], and many glaciers terminate offshore, where calving provides an efficient mass sink through which ice loss is translated rapidly into sea-level rise. However, most current models used to project the contribution to sea level from the High Arctic's land ice do not incorporate any dynamic feedbacks in response to increased melt rates [*Alley et al.*, 2005; *IPCC*, 2007; *Rignot and Kanagaratnam*, 2006], due in part to limited knowledge of the mechanism(s) by which supraglacial water penetrates to the base and induce(s) a dynamic response. Rare exceptions to date are *Parizek and Alley*'s [2004] simulations of the Greenland Ice Sheet's response to three different global warming scenarios incorporating seasonally-enhanced basal motion, and *Pattyn et al.*'s [2005] model of polythermal McCall Glacier, Alaska, which highlights the potential significance of basal motion for the annual flow regime.

45 Recent research by *van der Veen* [2007] has shown theoretically that supraglacial-subglacial
46 connections can be established through ice several hundreds of metres thick over periods of only
47 a few hours by the water-driven propagation of crevasses. This requires the ice to be under tensile
48 stress and crevasse-filling rates of at least 1 m $hr^{-1}$, most feasibly attained by surface water
49 ponding into supraglacial lakes overlying the crevasses before they begin to propagate
50 downwards [*van der Veen*, 2007]. The mechanism has been observed directly at John Evans
51 Glacier, Canada [*Boon and Sharp*, 2003]; and satellite observations of supraglacial lakes forming
52 and draining seasonally over the Greenland Ice Sheet imply its wider occurrence [*McMillan et*
53 *al.*, 2007; *Sneed and Hamilton*, 2007]. These findings confirm that supraglacial hydraulic forcing
54 is likely in the High Arctic, but the requirement for surface water to overcome the thermal barrier
55 of cold ice at the surface means it occurs via far fewer and more widely spaced supraglacial-
56 subglacial connections than on temperate glaciers. In a typical temperate glacier, supraglacial
57 hydraulic forcing causes speedups in basal motion where supraglacial inputs locally reduce basal
58 traction; this then alters the stress fields in the surrounding ice, such that the initial speedup is
59 transmitted through the ice to the surface and adjacent regions by stress-gradient coupling
60 [*Blatter et al.*, 1998; *Nienow et al.*, 2006]. What remains unclear in High Arctic ice masses is the
61 extent to which meltwater inputs limited to fewer and more widely spaced locations can cause
62 either localised or more spatially extensive speedup events.
63
64 In this paper, we investigate seasonal variations in the distribution of basal sliding under a
65 polythermal (predominantly cold) High Arctic glacier, and their effects on the overall flow
66 regime. More specifically, we use an existing three-dimensional, finite-difference glacier flow
67 model [*Blatter*, 1995; *Hubbard et al.*, 1998] to assess the extent to which localised perturbations
68 in basal traction, such as those typically provided by supraglacial hydraulic forcing, can be
69 transmitted through such a glacier by stress-gradient coupling, particularly along the
70 (longitudinal) direction of the main flow-line. We apply the model to John Evans Glacier,

71 Nunavut, Canada, where detailed field measurements of ice motion and hydrology were obtained
72 between 1994 and 2002. In doing so, we aim to improve the current understanding of the length-
73 scales of stress-gradient coupling in predominantly cold ice masses, which has important
74 implications for the response of High Arctic glaciers and the Greenland Ice Sheet to supraglacial
75 hydraulic forcing.
76

## BACKGROUND AND METHODOLOGY

### Physical setting

John Evans Glacier (79°40'N, 74°00'W; hereafter JEG) covers 165 $km^2$ and flows 15 km from an altitude of 1500 m to terminate on land at 100 m a.s.l. near the head of Allman Bay, eastern Ellesmere Island (Fig. 1a). Ground-based radio-echo sounding (RES), conducted at 3200 points across the glacier, has been used to determine its thickness and basal thermal conditions [*Copland and Sharp*, 2001]. Over the lower ablation zone (LABZ; 0-5 km above the terminus), the lower accumulation zone (LACZ; 8-11 km above the terminus) and the upper accumulation zone (UACZ; 11-15 km above the terminus), ice is typically 100-200 m thick. Over the upper ablation zone (UABZ; 5-8 km above the terminus) ice attains depths up to 400 m, and flows across an overdeepened trough (Fig. 1b). At the upper boundary of the UABZ, i.e. approximately at the equilibrium-line altitude (ELA; 8 km above the terminus and 800 m a.s.l.), ice flows either side of a nunatak, while at the lower limit of the UABZ (4 km above the terminus) the ice thins significantly over a subglacial bedrock riegel (Fig. 1b). Thermal conditions were determined by analysing all traces for residual bed reflection power ($BRP_r$), the bed reflection power corrected for ice thickness, for which values >1 generally indicate warm basal ice (after *Gades et al.*, [2000]). Over most of the ablation zone – but not at the margins and terminus - high $BRP_r$ (Fig. 1c) indicates warm basal ice. In the LABZ an internal reflector up to 40 m above the bed was interpreted as the boundary between warm basal ice and cold overlying ice [*Copland and Sharp*, 2001]. Throughout the whole accumulation zone and over the margins, terminus and riegel, low $BRP_r$ (Fig. 1c) implies cold basal ice. Thermistors emplaced 15 m below the ice surface across the glacier yielded values ranging from -9.5 to -15.1º C (Fig. 1c), confirming that surface ice remains cold all year round. Results from the radar survey therefore suggest the glacier is polythermal but almost entirely cold, with warm ice only detected at and near the ice-bed

interface within the ablation zone (Fig. 1d). Hereafter we use the phrase 'predominantly cold' to describe the thermal regime of JEG, to distinguish it amongst the full continuum of polythermal regimes which can exhibit widely contrasting hydrology/dynamics relationships (see *Blatter and Hutter* [1991] for a range of polythermal regimes; JEG manifests the form shown in their Fig. 1d).

**Observed motion patterns**

Measurements of glacier surface motion between 1998 and 2002 [*Bingham et al.*, 2003; *Copland et al.*, 2003b] reveal an annual pattern of ice motion with fastest flow (~20 m $a^{-1}$) in the LABZ (Fig. 2a). Superimposed onto this pattern is a more complex picture of glacier-wide seasonal variations in ice motion (Fig. 2b-d). In particular, we identify three key periods of the year over which distinct motion distributions are observed (as reported in more detail in *Bingham et al.*, [2003]). These periods may be summarised as follows:

(i) *Winter* (September – May; Fig. 2b). During this period, there is very little, if any, surface melting, no surface runoff reaches the base, and there is no subglacial outflow. Ice flows more slowly at this time of year across all parts of the glacier than at any other time.

(ii) *Spring* (mid-late June; Fig. 2c). Over the month preceding this period, surface melt is generated down-glacier of the ELA. In the LABZ it drains over the surface to the margins, but in the UABZ most drains instead into a series of surface ponds. The beginning of '*spring*' is defined by the sudden drainage of these surface melt-ponds into the glacier interior via five moulins that open over the riegel at the lower limit of the UABZ (h1-h5, Fig. 1a; also cf. Fig. 2c), and a corresponding outburst of meltwater from the subglacial outlet at the terminus which typically occurs 1-2 days later. Surface motion across the LABZ dramatically increases at this time, often exceeding twice the mean annual speed during the first 2-3 days [*Copland et al.*, 2003a; *Bingham et al.*, 2006], after which it slows

but remains around 1.2-1.5 times winter speeds. Surface motion also increases over the UABZ and the LACZ, but no increase in surface motion is observed over the UACZ.

(iii) *Summer* (July; Fig. 2d). During this period, the snowline retreats into the UACZ, and surface runoff occurs widely across the glacier. Supraglacial melt continues to drain into the five riegel moulins (h1-h5), but much up-glacier melt now drains into the glacier interior via two further moulins (h6 and h7) which open 11 km above the terminus (i.e. defining the boundary between the LACZ and the UACZ). Peak seasonal flow velocities are observed throughout the UABZ and LACZ; flow increases above winter levels in the UACZ; and high flow continues across the LABZ.

The higher velocities observed across the glacier during spring and summer undoubtedly result from supraglacial hydraulic forcing. In particular, faster ice motion through the LABZ during spring is associated with widespread surface uplift over the same region [*Copland et al.*, 2003a; *Bingham et al.*, 2006], and is consistent with surface melt suddenly gaining access to an inefficient subglacial drainage system via the freshly-opened riegel moulins [*Bingham et al.*, 2005]. However, what is not clear is the extent to which this localised dynamic response down-glacier of the riegel is transmitted up-glacier through stress-gradient coupling. *Copland et al.* [2003b], using a single flow-line model, postulated that supraglacial hydraulic forcing beneath the LABZ was sufficient to draw down ice from the accumulation zone provided the longitudinal coupling length exceeded 4 times the ice thickness. They supported this assertion with the theoretical inference that longitudinal coupling is significantly more effective in cold ice than temperate ice [*Kamb and Echelmeyer*, 1986]. Since that interpretation, however, a number of issues have arisen. Firstly, *Copland et al.* [2003b] compared winter motion only with 'summer' motion, where their definition of 'summer' comprised an amalgamated period combining the spring and summer periods we have defined above. As we have seen, the glacier's dynamic response, and probably therefore the nature of its forcing/coupling mechanisms, evolves

154 markedly as the melt season progresses, most notably up-glacier of the LABZ (cf. Figs. 2c and
155 2d). Secondly, they neglected the existence of the accumulation zone moulins (h6 and h7 at the
156 head of the LACZ), whose connectivity to the subglacial outlet has been confirmed by dye
157 tracing [*Bingham et al.*, 2005]. The existence of these higher-altitude moulins raises the
158 possibility that supraglacial hydraulic forcing may impact directly on basal sliding some way up-
159 glacier of the riegel moulins (i.e. across the LACZ and/or the UABZ), so that we do not
160 necessarily need to appeal to extensive longitudinal coupling with supraglacial hydraulic forcing
161 further down-glacier (as do *Copland et al.* [2003b]). Finally, *Bingham et al.* [2005] have
162 demonstrated that the subglacial drainage system beneath the LABZ can evolve rapidly into a
163 highly efficient configuration in the days following the spring event, reducing the impact of
164 supraglacial hydraulic forcing on basal motion across the LABZ later in the summer.
165
166 Here we attempt to resolve the seasonal distribution of basal sliding, and reassess the possible
167 glacier-wide impact of localised perturbations in basal sliding rate via longitudinal stresses, using
168 a fully three-dimensional, finite-difference model of glacier flow with a mixed thermal regime.
169
170 **Model description**
171
172 The model is based on that developed by *Blatter* [1995], which provides first-order solutions to
173 the mass- and force-balance equations for three-dimensional grounded ice masses in steady state.
174 Model derivation, numerical implementation, proof through comparison with an idealised case
175 solution, and its application to studying basal motion beneath the temperate Haut Glacier d'Arolla
176 are given by *Blatter* [1995], *Blatter et al.* (1998), *Colinge and Blatter* [1998], *Hubbard et al.*
177 [1998] and *Nienow et al.* [2005] respectively. The model has been validated in a recent Ice Sheet
178 Model Intercomparison Project for Higher-Order Models [ISMIP-HOM; *Pattyn et al.*, 2007] for
179 both real and hypothetical glacier geometries with a variety of fixed and mixed basal boundary

conditions. It calculates longitudinal and lateral stress gradients, handles a nonlinear constitutive relation and calculates the steady state stress and velocity fields for a given geometry and a prescribed velocity or traction distribution at the glacier bed and a vanishing shear traction at the surface. It does not explicitly incorporate a physical description of the mechanisms that induce spatial variations in basal drag (such as supraglacial hydraulic forcing); rather, the model is used heuristically to derive the thermal and basal motion fields that replicate the observed surface flow fields, and interpret the likely mechanisms which may bring about the optimum basal velocities retrospectively in the context of the field observations described above.

The model is fully thermodynamic and the computed three-dimensional stress field is coupled to strain-rates through a constitutive relation which takes the form of Glen's law given by:

$$D = A\left(I_{\Pi} + t_0\right)^{(n-1)/2} \Sigma$$

where $D$ is the strain rate tensor, $A$ is the 'rate factor', $I_{\Pi}$ is the second invariant of the stress deviator ($\Sigma$), $n$ is the flow law exponent (taken as 3), and $t_0$ is a nominally small constant which ensures a finite viscosity is retained when approaching the limit of zero stress at ice divides [*Blatter*, 1995]. Specifically, the thermal regime couples to the rate factor, $A$, which can be treated as a constant for isothermal conditions, or can vary as a function of temperature (or other physical qualities) following the Arrhenius relation [*Paterson*, 1994, p. 86]. For simulating polythermal conditions, the model calculates the three-dimensional temperature field based on horizontal and vertical advection, conduction and internal strain and basal frictional heating which are explicitly coupled to the mechanical component. Upper and lower boundary conditions are provided by the mean annual surface temperature (obtained from thermistor measurements 15 m beneath the glacier surface; Fig. 1c) and the geothermal heat flux which is assumed constant across the bed. The thermal component of the model is spun-up under an initial condition of isothermal ice (~-10°C) which is iterated through time in consort with the ice mechanics until the thermomechanical regime attains equilibrium. Sensitivity experiments reveal that the result is

robust and independent of the initial spin-up condition, though initiating with colder (~-12°C) rather than warmer ice leads to a quicker steady-state solution.

The model requires six inputs: bed and surface slopes, surface temperature, ice thickness, the basal motion field and the geothermal heat flux. The model is run at 250 m horizontal grid resolution, with the glacier geometry (thickness and slopes) derived directly from the bed and surface DEMs produced by *Copland and Sharp* [2001] and kept constant for all the experiments presented. The model solves the coupled thermal and mechanical components in consort by integrating vertically from the bed to the surface using a second-order Runge-Kutta scheme to satisfy the surface boundary condition of negligible shear stress, and the unknown basal shear traction is modified using a fixed-point iteration scheme [*Hubbard et al.*, 1998]. The computed steady-state thermal and velocity fields generated are then compared with the field measurements made at JEG.

**Control experiments**

Before proceeding with the main series of modelling experiments, two control runs were conducted in which basal motion was precluded (i.e. basal motion was prescribed as zero), and only thermal conditions were allowed to alter. The aim was to discern whether the model could simulate observed surface motion at any time without recourse to basal motion. As an initial control (JEG01), the model was applied in temperate isothermal mode, equivalent to raising all ice to pressure-melting point (PMP) by specifying a constant rate factor for temperate ice ($A$ = $2.148 \times 10^{-16}$ $kPa^{-3}$ $a^{-1}$; Paterson, 1994, p.97) across the entire domain. The objective of JEG01 was to determine the highest velocities that could be accounted for by internal deformation alone, taking the extreme (and unrealistic) end-member that JEG is temperate and isothermal. In other

words, it tests the degree to which warming the ice, rather than introducing basal motion, would be reflected in surface ice flow.

The steady-state surface velocity field produced by experiment JEG01 is shown in Fig. 3a. Significantly, modelled surface velocities through much of the ablation zone remain close to or below those observed at any time of year (Fig. 3b), even during winter, when the slowest surface motion is recorded (Fig. 3c). Thus, even by raising all ice to pressure-melting point we cannot account for the observed magnitudes of ice motion through the ablation zone by appealing to internal deformation alone, hence another mechanism must be responsible. By apparent contrast, across much of the accumulation zone the temperate and isothermal experiment massively overestimates ice flow (Fig. 3a & c). This is not especially meaningful, however, because we know that in reality ice throughout the accumulation zone is almost entirely cold, and therefore will experience much lower rates of deformation than are implied by this isothermal run. It does demonstrate, however, that internal deformation is highly sensitive to the thermal evolution, and so it is necessary to investigate more realistic thermal boundary conditions.

We therefore ran a second control experiment, JEG02, with zero basal motion but a fully evolved steady-state polythermal regime. We prescribed surface temperatures across the glacier ranging between -12 and -10°C, based on the 15-m thermistor measurements made during the field observations (Fig. 1c), and set a value of 60 mW $m^{-2}$ for the geothermal heat-flux after direct measurements made at the similar geophysical setting of Barnes Ice Cap, Baffin Island [*Classen*, 1977].

The steady-state surface velocity field (contoured) and basal temperature field (graduated shading) derived by JEG02 are shown in Fig. 3b. JEG02 demonstrates two things. Firstly, in terms of the glacier's dynamics, it reveals that with no basal motion, surface velocities are

underestimated across all parts of the glacier regardless of the time of year. Modelled surface velocities across the LABZ are 2-4 times lower than observed over winter and an order of magnitude lower than those observed over summer (Fig. 3c); and modelled surface velocities across the accumulation zone similarly underestimate observed speeds (Fig. 3b & c). JEG02, in combination with JEG01, therefore strongly suggests that significant basal motion must be occurring across zones of this predominantly cold glacier. Secondly, in terms of the glacier's thermal conditions, JEG02 evolves a steady-state basal temperature field (Fig. 3b) that reasonably approximates that measured by RES (cf. Fig. 1c), with colder basal ice in the accumulation zone than in the ablation zone (Fig. 3c). However, nowhere in the ablation zone do basal temperatures in JEG02 attain PMP. This may be because the geothermal heat flux we specify (60 mW $m^{-2}$) is too low, although the region's geology and longstanding tectonic stability (Hodgson and others, 1989) provide no evidence that geothermal heating in this region should be significantly higher. Furthermore, sensitivity experiments indicate that even with geothermal heat flux increased by a factor of 50% to 90 mW $m^{-2}$, nowhere does the bed of JEG attain PMP under equilibrium conditions with basal motion precluded. A more tangible explanation could be that the heat deficit results from the model not accounting for sensible heat transferred by water from the surface to the bed, and the frictional heating that results from en- and subglacial water flow. Such frictional heating is probably an important heat source throughout at least the LABZ, where RES indicates warm basal ice and supraglacial hydraulic forcing is known to occur [*Bingham et al.*, 2005]. We therefore believe that the thermal conditions used to force JEG02 represent a good thermal model within the limits of this study.

Thus, we used the control runs described above to determine reasonable thermal conditions for the model, and to confirm that basal motion is required beneath all or part of JEG to replicate the observed surface motion fields through all parts of the year. The main series of modelling runs we describe below was therefore designed to determine the degree to which basal motion is

required to replicate the observed surface motion fields at different times of the year, and to assess to what degree the required forcing can be localised around supraglacial inputs or may be transmitted to adjacent regions of the glacier through stress-gradient coupling.

**Modelling experiments**

In the following series of experiments, we used the same thermal inputs as those used for JEG02, but varied the magnitude of basal forcing and the areas over which it is active for different times of year. We estimated the magnitude of basal forcing over given periods based on the differences between observed surface motion fields (Figs. 2b-d) and the modelled surface motion field resulting from no basal motion (JEG02; Fig. 3b). This makes the implicit assumption that any measured surface motion over any given period that exceeds that produced by JEG02 at steady state is a direct surface expression of enhanced basal motion. We thereby derived 'residual' winter, spring and summer basal motion fields by subtracting the JEG02 surface motion field (Fig. 3b) from the winter, spring and summer surface motion fields (Figs. 2b-d) respectively.

We performed five numerical experiments, as follows:

JEG03 was forced with 'residual winter' motion (Fig. 4a), i.e. the residual of Fig. 3b and Fig. 2b. The rationale was to investigate the degree to which surface velocities observed across the glacier over winter may result from a basal component of motion.

JEG04 was forced with 'residual summer' motion (Fig. 4b), i.e. the residual of Fig. 3b and Fig. 2d. The rationale for this experiment was to investigate whether the faster velocities observed over the glacier during summer may adequately be explained by increasing the basal component relative to winter, such as might result from supraglacial hydraulic forcing.

JEG03 and JEG04 assume basal motion is ubiquitous. However, given the highly localised nature of the supraglacial-subglacial connections we have observed, and the relatively short periods over which they are active (1-2 months per year), it may be more reasonable to suppose that when supraglacial hydraulic forcing is taking place (i.e. during spring and summer), the resultant basal forcing is concentrated around and downstream from supraglacial input locations. Therefore, in experiments JEG05, JEG06, and JEG07, we test the effects of prescribing only partial basal motion fields across selected zones of JEG during spring and summer:

JEG05 was forced with 'residual spring' basal motion *only across the LABZ* (Fig. 5a). The rationale for this experiment was to investigate (i) the effect of a localised increase in basal forcing beneath the LABZ, over a period when we know localised supraglacial hydraulic forcing is taking place due to meltwater inputs into moulins h1-h5 (Fig. 1a), and (ii) the degree to which this localised excess ice flow can be transmitted up-glacier through longitudinal coupling alone. We consider the spring period for this test because this is when peak velocities are observed across the LABZ, so we would expect up-glacier stress-gradient coupling to be at its strongest.

JEG06 was similar to JEG05, but with the active basal motion field extended up-glacier to the head of the UABZ (Fig. 5b). This represents the known up-glacier limit of warm basal ice [*Copland and Sharp*, 2001], hence the up-glacier limit of any expected basal motion, although no supraglacial inputs have been observed up-glacier of the LABZ during spring. Here again we test the efficacy of longitudinal coupling, by testing whether expanding the limit of basal motion up-glacier has any positive effect on ice motion through the cold accumulation zone.

334 JEG07 was forced with 'residual summer' basal motion *only across the UABZ* (Fig. 5c). This
335 reflects our expectation that later in the melt season the region of highest basal forcing may
336 migrate up-glacier from the LABZ to the UABZ due to (i) the onset of drainage into the
337 accumulation-zone moulins (h6 and h7, Fig. 1a), delivering surface runoff that might first
338 encounter warm basal ice at the head of the UABZ, and (ii) the increased efficiency of
339 subglacial drainage through the LABZ evident by July [after *Bingham and others*, 2005],
340 which would act to dampen basal forcing down-glacier of the UABZ.
341

## RESULTS

Figure 4 shows the results from model experiments JEG03 and JEG04, respectively forced with residual winter (Fig. 4a) and residual summer (Fig. 4b) basal motion fields. The attempt to reproduce the winter surface motion field (JEG03; Fig. 4a) replicates well the general dynamic behaviour observed at the surface, although along the glacier centreline surface velocities are generally slightly underestimated (Fig. 4c). At steady state, warmer basal temperatures are found more generally in the LABZ than elsewhere (Fig. 4a), although for the most part the base remains well below melting point and nowhere is the modelled basal temperature field at melting point. The attempt to reproduce the summer surface motion field (JEG04; Fig. 4b) also performs reasonably in terms of the basic pattern, simulating the increase in velocities observed across much of the surface with respect to winter. Along the glacier centreline (Fig. 4c) the model generally underestimates the observed surface velocity by 15-30% (3 – 7 m $a^{-1}$), except in the LABZ, where the observed summer flow is overestimated by 60% (15 m $a^{-1}$), and in the lowest 2 km, where it is underestimated by 15% (~ 3 m $a^{-1}$). The increased flow through most of the glacier warms more of the base (Fig. 4b) than in the winter model (Fig. 4a), with a greater proportion of the ablation zone at warmer basal temperatures. Nevertheless, PMP is still not attained anywhere at the glacier base.

Figure 5 shows the results from experiments where only partial basal forcing fields were prescribed. JEG05 and JEG06, forced with residual spring basal motion only in the LABZ (Fig. 5a) and only down-glacier of the nunatak (Fig. 5b) respectively, both reproduce well the observed dynamic behaviour in spring wherever basal motion is prescribed (Fig. 5d). Notably, as soon as the boundary into the zero basal motion field is crossed (i.e. up-glacier of the riegel in JEG05 and up-glacier of the nunatak in JEG06) each model significantly underestimates observed flow. This conclusion is also valid for JEG07 (Fig. 5c), in which surface velocities are massively

underestimated (relative to those observed in summer) in the LABZ where zero basal motion was prescribed. The most significant finding from these three models is that wherever zero basal motion is prescribed, the local surface velocity response fails to attain the observed magnitudes (Fig. 5d); the implication is that high velocities at the surface result from locally high rates of basal motion, rather than from stress-gradient coupling. This is highlighted by the failure of all three models to replicate observed velocities in the accumulation zone through stress-gradient coupling alone. Once again, it is also notable that although the modelled basal temperature fields reproduce the general pattern of observed variation in $BRP_r$, nowhere does even the warmest modelled basal ice quite reach pressure-melting point (Figs. 5a-c).

## DISCUSSION

Our model results support the contention, based on earlier field observations, that a substantial component of the annual flow of JEG results from basal motion, despite the prevalence of cold ice throughout much of the glacier. It is notable that regardless of the time of year, and even when the temperature of all the ice is raised to PMP - significantly increasing the internal deformation rate – a considerable basal perturbation is required in the ablation zone for the observed surface velocities to be modelled. These findings are entirely consistent with our field observations that basal ice in the ablation zone is at PMP, permitting basal motion, and that during spring and summer basal motion beneath the ablation zone is enhanced by supraglacial hydraulic forcing. We have also learnt that even during winter a significant basal motion component is required beneath the ablation zone, and that during spring and summer basal motion is likely beneath the LACZ.

Critically, the modelling suggests that almost all excess motion observed at the surface is a direct expression of local basal motion, and in particular the effect of stress-gradient coupling on transmitting basal motion anomalies up-glacier is muted. The evidence for minimal longitudinal coupling is provided by those experiments (JEG05-07; Fig. 5) where we restricted basal forcing to localised sectors of the bed. Enhancing basal motion only across the LABZ during spring (JEG05; Fig. 5a), when the most pronounced surface speedup is observed across the LABZ, causes a negligible increase in surface flow up-glacier, and does not induce an increase in surface motion in the accumulation zone. Expanding the basal motion field up-glacier additionally to incorporate the UABZ (JEG06; Fig. 5b) also has a negligible effect on ice flow in the accumulation zone, and even raising basal motion beneath the UABZ to the maximum summer levels (JEG07; Fig. 5c) fails to increase flow up-glacier of the ablation zone. Our findings therefore do not support the contention of *Copland et al.* [2003b], derived from 2-dimensional

(flowline) modelling, that JEG has a longitudinal coupling length of 4 times the local ice thickness. This has three implications: firstly, significantly different conclusions can be drawn concerning the efficacy of longitudinal coupling depending on whether modelling is conducted in two or three dimensions; secondly, we need to explain why stress-gradient coupling is less effective than suggested by *Copland et al.* [2003b]; and thirdly, the high motion observed in the accumulation zone likely results directly from basal motion in the accumulation zone suggesting that at least part of the bed in this region is at PMP.

Earlier research at the temperate Haut Glacier d'Arolla, Switzerland, has highlighted the possibility of overestimating the effectiveness of stress-gradient coupling using a flowline model rather than a three-dimensional model. *Blatter et al.* [1998] applied a flowline model to the glacier which derived a longitudinal coupling length-scale of 3-5 times the ice thickness; but the same formulation incorporated into a three-dimensional model [*Nienow et al.*, 2005] suggested that up-glacier coupling actually occurred over distances of less than one ice thickness. The discrepancy may arise for a number of reasons. In the Arolla work, it was suggested that transverse stresses, not taken into account by single flow-line models, significantly reduce the efficacy of longitudinal stress-gradient coupling, effectively producing a rapid longitudinal dissipation of supraglacially-forced basal motion anomalies [*Nienow et al.*, 2005]. Lateral variations in basal drag, such as might be imposed by 'sticky' patches of basal ice away from a subglacial channel, or by friction against valley walls, are also neglected in the two dimensional case. At JEG, patches of cold basal ice may additionally act as significant sticky spots. JEG also flows over, and/or around, at least two significant topographic pinning points, the riegel between the LABZ and the UABZ, and the nunatak between the UABZ and the LACZ, and these might also suppress longitudinal stress-gradient coupling.

427 Our conclusion that stress-gradient coupling is ineffective at transmitting down-glacier basal
428 motion anomalies up-glacier of the nunatak suggests that basal motion must be responsible for
429 the significant speedup observed during summer in the LACZ. This means that we must reconcile
430 the existence of basal motion there with RES data that suggest the basal interface is cold (Fig.
431 1c). The most likely explanation is that at least some parts of the basal interface in the LACZ are
432 at PMP, and were not detected by RES. This raises two issues: firstly, how may warm basal ice
433 be generated beneath the LACZ despite modelled thermal conditions to the contrary, and
434 secondly, why was it not detected during RES surveying? On the first point, some 'relict' warm
435 basal ice may survive from a period of thicker glacial cover, when ice thickness in the LACZ was
436 sufficient to raise basal ice to pressure melting point and insulate it from the cold climate above.
437 This same argument has been put forward to explain anomalous warm sectors of polythermal
438 Laika Glacier, Canadian Arctic [*Blatter and Hutter*, 1991], and McCall Glacier, Alaska [*Pattyn et*
439 *al.*, 2005]. Alternatively, or in addition, heat supplied by surface runoff accessing the subglacial
440 interface (e.g. through moulins h6 and h7) may maintain parts of the basal interface at pressure
441 melting point. On the potential failure of the RES technique to identify warm ice beneath the
442 accumulation zone, the interpretation of high $BRP_r$ as a reliable indicator of cold ice may be
443 overstated, or it is possible that the RES coverage simply missed areas of warm ice.
444
445 As with any modelling exercise, our study has limitations that future efforts must address. Firstly,
446 while we have modelled the effect of perturbing basal motion fields on surface motion, we have
447 not explicitly incorporated the mechanism responsible for perturbing the basal motion fields in
448 the first place, i.e. the supraglacial hydraulic forcing mechanism. This requires an incorporation
449 of fracture mechanics into the ice-flow component which was beyond the scope of this study, but
450 which should be incorporated into an improved holistic formulation of the system. Secondly,
451 although we have reproduced well the general pattern of basal temperature variation over the
452 glacier as determined from RES, our modelling has shown a general tendency to underestimate

453 basal temperatures such that PMP was not attained anywhere at the base. As discussed in relation
454 to control experiment JEG02, we attribute the discrepancy to the model not incorporating heat
455 supplied to the base by seasonal inputs of water, and frictional heating generated by this water as
456 it melts a passage beneath the glacier. Therefore, future simulations might be improved with an
457 explicit incorporation of a water-derived heat expression. Finally, there may be a problem in
458 assuming that longitudinal coupling only affects the deformational component of flow. It seems
459 intuitive that it will also affect the rate of basal sliding with the potential that local perturbations
460 in basal traction could propagate velocity perturbations over greater distances than suggested by
461 our modelling. Unfortunately, there is currently no theoretical basis for addressing this issue and
462 it is a problem inherent to all higher order ice flow models.
463
464 **Wider implications for the dynamic response of High Arctic land ice to climate warming**
465
466 The findings from this study have a number of wider implications for predicting the likely
467 response of High Arctic ice masses, including the Greenland Ice Sheet, to projected climate
468 warming. The recent Fourth Assessment report of the *IPCC* [2007] has suggested that dynamic
469 processes related to ice flow could increase the vulnerability of the ice sheets to warming, but
470 effectively incorporating these processes into models remains one of the greatest challenges in
471 predicting the future contribution of ice sheets to sea level. The same point is equally applicable
472 to the smaller High Arctic glaciers and ice caps, which are also responding rapidly to climate
473 warming and are also contributing to rising sea levels. As we have noted, seasonal speedups have
474 been observed and attributed to supraglacial hydraulic forcing at a number of High Arctic glaciers
475 [*Bingham et al.*, 2003; *Müller and Iken*, 1973; *Rippin et al.*, 2005], but it has been difficult to
476 apportion the surface response between localised basal motion and stress-gradient coupling with
477 a non-local basal anomaly. Longitudinal stress-gradient coupling has generally been considered
478 more effective in colder ice [*Copland et al.*, 2003b; *Kamb and Echelmeyer*, 1986], and this has

been used to suggest that even small amounts of basal forcing in one location can drive a widespread speedup through a large proportion of an ice mass. This is a serious concern taken in the context that summers across the High Arctic are becoming longer and warmer, generating larger volumes of surface runoff over longer periods, and increasing the number and duration of supraglacial-subglacial hydraulic connections. However, our study suggests that other factors, such as lateral variations in basal drag, or the presence of topographic pinning points, significantly reduce the efficacy of longitudinal coupling, at least in a valley-glacier setting, and limit the dynamic response to localised areas of supraglacial hydraulic forcing.

Our study also underlines the importance of incorporating basal motion into models predicting the response of High Arctic glaciers and the Greenland Ice Sheet to climate warming. Clearly, at JEG, despite the vast majority of the ice being cold, a significant proportion of the ice flow results directly from basal motion. Only by including this basal motion in our model can we simulate the current flow regime at the glacier, hence any study seeking to project the response of High Arctic glaciers to climate warming must incorporate at the very least a sliding 'law', if not a more complex incorporation of subglacial processes, and should take into account supraglacial hydraulic forcing. Seasonal speedups observed on Greenland outlet glaciers [*Joughin et al.*, 1996; *Mohr et al.*, 1998] also suggest they have a warm basal interface, and therefore that basal motion is an important dynamic process at least at the fringes of the continental ice sheet. Recently it has come to light that many of Greenland's outlet glaciers are accelerating over annual/decadal timescales [*Howat et al.*, 2005; *Luckman et al.*, 2006; *Rignot and Kanagaratnam*, 2006; *Stearns and Hamilton*, 2007], and many possible causes for this phenomenon have been proposed, including an increased influence of supraglacial hydraulic forcing [*Zwally et al.*, 2002], or oceanic warming [*Payne et al.*, 2005], leading to ice-shelf removal and/or ice-front retreat, reducing resistance to flow. Whatever the catalyst(s) for these marked accelerations, it is certain that beneath Greenland's outlet glaciers much basal ice is warm, thus basal motion forms a

505 significant component of the dynamic response and must be incorporated into models seeking to
506 project the response of *all* High Arctic land ice to climatic warming.
507
508

## CONCLUSIONS

John Evans Glacier experiences significant seasonal increases in surface velocity every melt season [*Bingham et al*., 2003]. This phenomenon has been linked to 'supraglacial hydraulic forcing,' whereby surface meltwater drains into a distributed subglacial drainage system, and induces enhanced basal motion across unspecified parts of the bed. What has remained unclear until now is the extent to which such a basal perturbation over one part of the bed may be transmitted more widely through the glacier through the effect of stress-gradient coupling. We have used a three-dimensional, thermally-coupled flow model incorporating stress-gradient coupling to investigate where, and by how much, the basal velocity field needs to be perturbed to reproduce the surface velocity fields at different times of the year. Prescribing zero basal motion in the model but varying thermal conditions, we were unable to simulate the surface velocity field at any time of year in all parts of the glacier except the upper accumulation zone. Hence, we infer that basal motion takes place downglacier of all known supraglacial-subglacial hydraulic connections during at least part of the year. By varying the magnitude and pattern of the basal velocity perturbation, the model was better able to replicate the observed surface velocity fields at different times of the year.

The modelling reported here implies that an earlier reported longitudinal coupling length-scale of 4 times the ice thickness for this mostly cold glacier, based on a single flow-line model [*Copland et al.*, 2003b], is a significant overestimate. Rather, by varying the areas of active basal motion at the bed, we have found that it is difficult to transmit basal motion anomalies up- glacier by more than one ice thickness, and in some sectors of the glacier the coupling length is severely reduced through the effect of topographic pinning points, especially around the nunatak marking the divide between the accumulation and ablation zones. This has two significant implications. Firstly, it shows that radically different estimates of the efficacy of longitudinal stress-gradient

coupling are obtained when modelling in three, as opposed to two, dimensions, and the former dramatically reduces the estimated longitudinal-coupling length scale relative to the latter. The reasons for this need to be further investigated, but the implication is that although longitudinal coupling has previously been stated to be more effective in colder ice masses, its role in transmitting basal motion anomalies over large distances may have been overstated. Hence, secondly, most surface velocity increases, such as those observed here, and at glaciers with comparable thermal regimes, probably arise directly from local basal forcing, and do not reflect stress-gradient coupling with non-local basal forcing. Recent studies have highlighted the neglect of potentially critical dynamic processes in models seeking to predict the contribution of High Arctic glaciers and the Greenland Ice Sheet to sea level rise. Our experiments highlight the importance of incorporating a basal motion component into future formulations.

**ACKNOWLEDGEMENTS**

This research was developed under the UK NERC-ARCICE programme. Fieldwork at John Evans Glacier was supported by NERC, NSERC, the University of Alberta Circumpolar Institute and Northern Science Training Programme, and the Geological Society of America, and was conducted with the kind permission of the communities of Grise Fjord and Resolute Bay. Field support and logistics were provided by the Polar Continental Shelf Project, Natural Resources Canada (PCSP/EPCP contribution number ######). We thank Heinz Blatter and an anonymous reviewer for careful reviews.

553 **REFERENCES**

554

555 Abdalati, W., and K. Steffen (2001) Greenland ice sheet melt extent: 1979-1999. *J. Geophys.*
556 *Res.*, *106*, 33983-33988.

557

558 Alley, R.B., T.K. Dupont, B.R. Parizek, and S. Anandakrishnan (2005), Access of surface
559 meltwater to beds of sub-freezing glaciers: preliminary insights. *Ann. Glaciol.*, *40*, 8-14.

560

561 Bingham, R.G., P.W, Nienow, and M.J. Sharp (2003), Intra-seasonal and intra-annual flow
562 dynamics of a High Arctic polythermal valley glacier, *Ann. Glaciol., 37*, 181-188.

563

564 Bingham, R.G., P.W. Nienow, M.J. Sharp, and S. Boon (2005), Subglacial drainage processes at
565 a High Arctic polythermal valley glacier, *J. Glaciol.*, *51*, 15-24.

566

567 Bingham, R.G., P.W. Nienow, M.J. Sharp, and L. Copland (2006), Hydrology and dynamics of a
568 polythermal (mostly cold) High Arctic glacier, *Earth Surf. Process. Landform.*, *31*, 1463-1479.

569

570 Blatter, H. (1995), Velocity and stress fields in grounded glaciers: a simple algorithm for
571 including deviatoric stress gradients, *J. Glaciol.*, *41*, 333-344.

572

573 Blatter, H., G.K.C. Clarke, and J. Colinge (1998), Stress and velocity fields in glaciers. Part II.
574 Sliding and basal stress distribution, *J. Glaciol.*, *44*, 457-466.

575

576 Blatter, H., and K. Hutter (1991), Polythermal conditions in Arctic glaciers, *J. Glaciol.*, *37*, 261-
577 269.

578

579 Boon, S. and M. Sharp (2003), The role of hydrologically-driven ice fracture in drainage system
580 evolution on an Arctic glacier, *Geophys. Res. Lett., 30*, 1916, doi:10.1029/2003GL018034.
581
582 Classen, D.F. (1977), Temperature profiles for the Barnes Ice Cap surge zone, *J. Glaciol.*, *18*,
583 391-405.
584
585 Colinge, J., and H. Blatter (1998), Stress and velocity fields in glaciers. Part I: Finite-difference
586 schemes for higher-order glacier models, *J. Glaciol.*, *44*, 448-456.
587
588 Copland, L., and M. Sharp (2001), Mapping hydrological and thermal conditions beneath a
589 polythermal glacier with radio-echo sounding, *J. Glaciol.*, *47*, 232-242.
590
591 Copland, L., M. Sharp, and P. Nienow (2003a), Links between short-term velocity variations and
592 the subglacial hydrology of a predominantly cold polythermal glacier, *J. Glaciol.*, *49*, 337-348.
593
594 Copland, L., M.J. Sharp, P.W. Nienow, and R.G. Bingham (2003b), The distribution of basal
595 motion beneath a High Arctic polythermal glacier, *J. Glaciol.*, *49*, 407-414.
596
597 Gades, A.M., C.F. Raymond, H. Conway, and R. Jacobel (2000), Bed properties of Siple Dome
598 and adjacent ice streams, West Antarctica, inferred from radio-echo sounding measurements, *J.*
599 *Glaciol.*, *46*, 88-94.
600
601 Hanna, E., P. Huybrechts, I. Janssons, J. Cappelen, K. Steffen, and A. Stephens (2005), Runoff
602 and mass balance of the Greenland Ice Sheet: 1958-2003, *J. Geophys. Res.*, *110*, D13108, doi:
603 10.1029/2004JD005641.
604

605 Howat, I.M., I. Joughin, S. Tulaczyk, and S. Gogineni (2005), Rapid retreat and acceleration of
606 Helheim Glacier, east Greenland, *Geophys. Res. Lett*., 32, L22502, *Geophys. Res. Lett*., 34,
607 L03501, doi: 10.1029/2006GL028697.
608
609 Hubbard, A., H. Blatter, P. Nienow, D. Mair, and B. Hubbard (1998) Comparison of a three-
610 dimensional model for glacier flow with field data from Haut Glacier d'Arolla, Switzerland, *J.*
611 *Glaciol.*, *44*, 368-378.
612
613 IPCC (Intergovernmental Panel on Climate Change) (2007), *Climate Change 2007: The Physical*
614 *Science Basis*, IPCC, Geneva, Switzerland.
615
616 Joughin, I., S. Tulaczyk, M. Fahnestock, and R. Kwok (1996), A mini-surge on the Ryder
617 Glacier, Greenland, observed by satellite radar interferometry, *Science*, *274*, 228-230.
618
619 Kamb, B., and K.A. Echelmeyer (1986), Stress-gradient coupling in glacier flow: I. Longitudinal
620 averaging of the influence of ice thickness and surface slope, *J. Glaciol.*, *32*, 267-284.
621
622 Luckman, A., T. Murray, R. de Lange, and E. Hanna, (2006), Rapid and synchronous ice-
623 dynamic changes in East Greenland, *Geophys. Res. Lett*., 33, L03503, *Geophys. Res. Lett*., 34,
624 L03501, doi:10.1029/2005GL025428.
625
626 McMillan, M., P. Nienow, A. Shepherd, and T. Benham (2007), Satellite investigations of the
627 seasonal evolution of supra-glacial lakes at the margins of the Greenland Ice Sheet, *Geophys.*
628 *Res. Abstracts*, *9*, 10940.
629

630 Mohr, J.J., N. Reeh, and S.N. Madsen (1998), Three-dimensional glacial flow and surface
631 elevation measured with radar interferometry, *Nature*, *391*, 273-276.
632
633 Müller, F., and A. Iken (1973), Velocity fluctuations and water regime of Arctic valley glaciers,
634 *International Association of Hydrological Sciences Publication*, *95*, 165-182.
635
636 Nienow, P.W., A.L. Hubbard, B.P. Hubbard, D.M. Chandler, D.W.F. Mair, M.J. Sharp, and I.C.
637 Willis (2005), Hydrological controls on diurnal ice flow variability in valley glaciers, *J. Geophys.*
638 *Res.*, *110*, F04002, doi:10. 1029/2003JF000112.
639
640 Parizek, B.R., and R.B. Alley (2004), Implications of increased Greenland surface melt under
641 global-warming scenarios: ice-sheet simulations. *Quat. Sci. Rev.*, *23*, 1013-1027.
642
643 Paterson, W.S.B. (1997), *The Physics of Glaciers, 3rd Edition*, Butterworth-Heinemann, Oxford.
644
645 Pattyn, F., and the ISMIP-HOM participants (2007), ISMIP-HOM: Results of the Higher-Order
646 Ice-Sheet Model Intercomparison exercise, *Geophys. Res. Abstracts*, *9*, 01351.
647
648 Pattyn, F., M. Nolan, B. Rabus, and S. Takahashi (2005), Localized basal motion of a
649 polythermal Arctic glacier: McCall Glacier, Alaska, USA, *Ann. Glaciol.*, *40*, 47-51.
650
651 Payne, A.J., P.R. Holland, A. Vieli, and D.L. Feltham (2005), Modelling the coupled evolution of
652 the ice shelf/stream flow system and the oceanic circulation in the ice-shelf cavity, *EOS Trans.*
653 *AGU*, *86*, C44A-01.
654

655 Rabus, B.T., and K.A. Echelmeyer (1997), The flow of a polythermal glacier: McCall Glacier,
656 Alaska, U.S.A., *J. Glaciol.*, *43*, 522-536.
657
658 Rignot, E., and P. Kanagaratnam (2006), Changes in the velocity structure of the Greenland Ice
659 Sheet, *Science*, *311*, 986-990.
660
661 Rippin, D.M., I.C. Willis, N.S. Arnold, A.J. Hodson, and M. Brinkhaus (2005), Spatial and
662 temporal variations in surface velocity and basal drag across the tongue of the polythermal glacier
663 midre Lovénbreen, Svalbard, *J. Glaciol.*, *51*, 588-600.
664
665 Sneed, W. A., and G.S. Hamilton (2007), Evolution of melt pond volume on the surface of the
666 Greenland Ice Sheet, *Geophys. Res. Lett*., 34, L03501, doi: 10.1029/2006GL028697.
667
668 Stearns, L.A., and G.S. Hamilton (2007), Rapid volume loss from two East Greenland outlet
669 glaciers quantified using repeat stereo satellite imagery, *Geophys. Res. Lett., 34*, L05503, doi:
670 10.1029/2006GL028902.
671
672 Steffen, K., S.V. Nghiem, R. Huff, and G. Neumann (2004), The melt anomaly of 2002 on the
673 Greenland Ice Sheet from active and passive microwave satellite observations. *Geophys. Res.*
674 *Lett.*, *31*, L20402, doi:10.1029/2004GL020444.
675
676 Van der Veen, C.J. (2007), Fracture propagation as a means of rapidly transferring surface
677 meltwater to the base of glaciers, *Geophys. Res. Lett.*, *34*, L01501, doi:10.1029/2006GL028385.
678
679 Zwally, H.J., W. Abdalati, T. Herring, K. Larson, J. Saba, and K. Steffen (2002), Surface melt-
680 induced acceleration of Greenland Ice-Sheet flow, *Science*, *297*, 218-222.
681

681 **Figure captions**

682

683 Figure 1: (a) Location map, showing the conceptual division of JEG into the upper accumulation
684 zone (UACZ), lower accumulation zone (LACZ), upper ablation zone (UABZ) and lower
685 ablation zone (LABZ). (b) DEM of bed elevation with RES lines superimposed. (c) Distribution
686 of residual bed reflection power ($BRP_r$); values >1 indicate warm basal ice, values <1 ice frozen
687 to the base. RES lines and 10-m depth thermistor measurements in °C are superimposed. (d)
688 Conceptual side-view of the glacier along the long profile in Fig. 2a, with important features
689 annotated.

690

691 Figure 2: (a) Annual surface velocity distribution, based on values measured between 1999 and
692 2001. Velocity stakes are shown as black dots; contours show velocity values interpolated onto a
693 200 m grid. Moulins that open during spring and summer are also shown. The red line shows the
694 glacier flow-line used for the glacier side-view in Fig. 1d and the long profile results in Figs. 3, 4
695 & 5. (b) Observed velocities over the 'winter' period between August 1999 and May 2000. The
696 contour field shows absolute values, while the colour scale is differenced with the annual
697 distribution. Inactive moulins are shown as crossed circles. (c) and (d) As for (b), but relating to
698 'spring' (June 2000) and 'summer' (July 2000) respectively.

699

700 Figure 3: Results from control experiments (a) JEG01 and (b) JEG02. LHS: basal temperature
701 (colour-scale) and surface-velocity (contours) at steady state; RHS: surface-velocity field relative
702 to the annual (colour-scale) with absolute velocities superimposed. (c) Velocity profiles along the
703 long profile shown in Fig. 2a for experiments JEG01 and JEG02, compared with observed values
704 in winter, spring and summer.

705

706 Figure 4: Results from experiments (a) JEG03 and (b) JEG04. The LHS shows the prescribed
707 basal forcing fields (contours) and basal temperature fields evolved at steady state; the RHS
708 shows the steady-state velocity fields both as absolute values (contours) and values relative to (a)
709 and (b) summer. (c) Velocity profiles along the long profile shown in Fig. 2a for experiments
710 JEG03 and JEG04, compared with observed values in winter and summer.
711
712 Figure 5: Results from experiments (a) JEG05, (b) JEG06 and (c) JEG07, in which basal forcing
713 was prescribed only beneath selected areas of the glacier. The LHS shows the prescribed basal
714 forcing fields (contours) and basal temperature fields evolved at steady state; the RHS shows the
715 steady-state velocity fields both as absolute values (contours) and values relative to (a & b) spring
716 and (c) summer. (d) Velocity profiles along the long profile shown in Fig. 2a for experiments
717 JEG05, JEG06 and JEG07, compared with observed values in spring and summer.

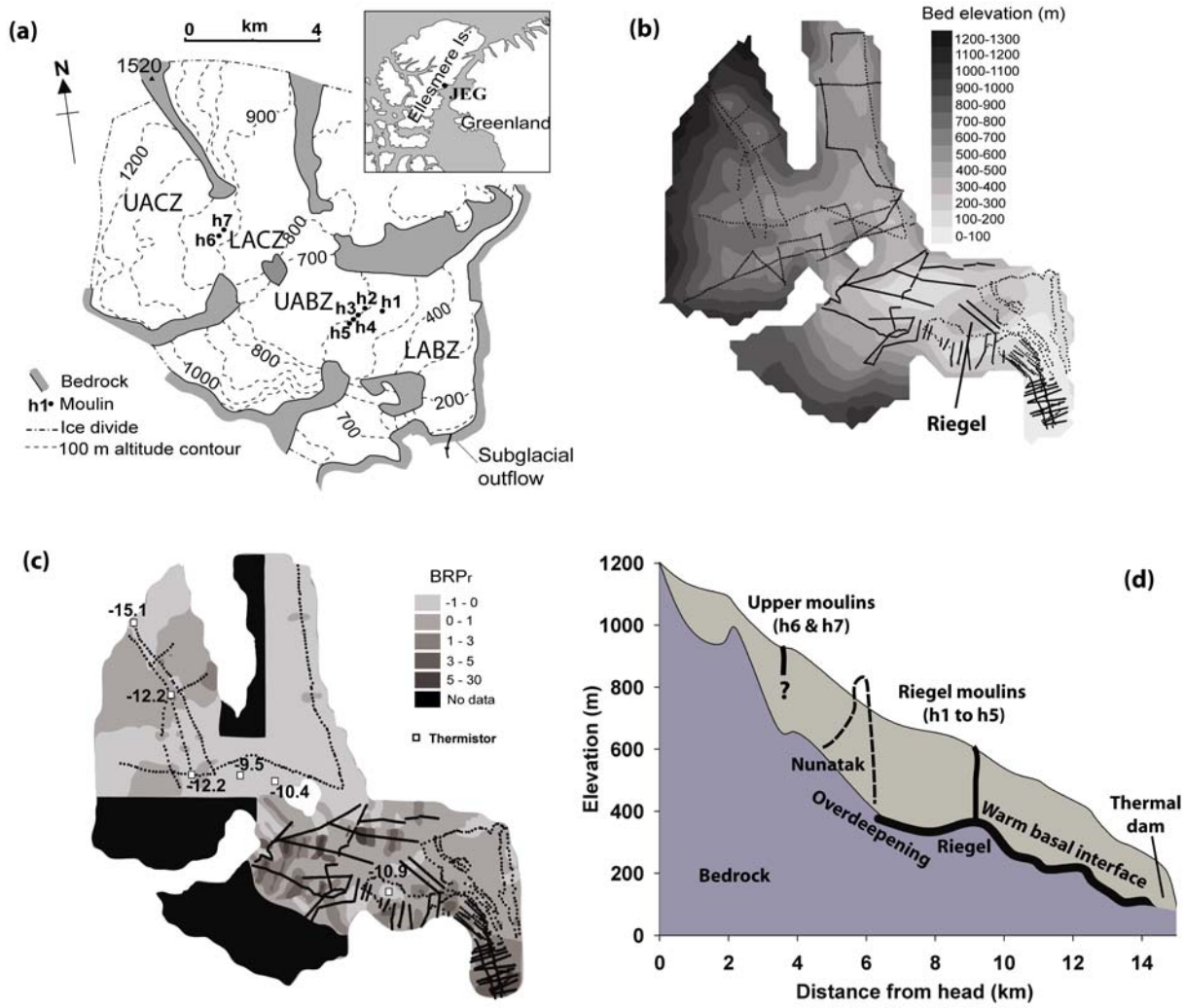
(a)
0 km 4
N
1520
900
1200
UACZ
h7
h6
LACZ
800
700
UABZ
h3
h2
h1
h5
h4
400
800
1000
LABZ
200
700
Bedrock
h1 Moulin
Ice divide
100 m altitude contour
Subglacial outflow
Ellesmere Is.
JEG
Greenland
(b)
Bed elevation (m)
1200-1300
1100-1200
1000-1100
900-1000
800-900
700-800
600-700
500-600
400-500
300-400
200-300
100-200
0-100
Riegel
(c)
BRPr
-1 - 0
0 - 1
1 - 3
3 - 5
5 - 30
No data
Thermistor
-15.1
-12.2
-9.5
-12.2
-10.4
-10.9
(d)
Upper moulins
(h6 & h7)
?
Riegel moulins
(h1 to h5)
Nunatak
Overdeepening
Riegel
Warm basal interface
Thermal
dam
Bedrock
Elevation (m)
Distance from head (km)
1200
1000
800
600
400
200
0
0
2
4
6
8
10
12
14

Figure 1

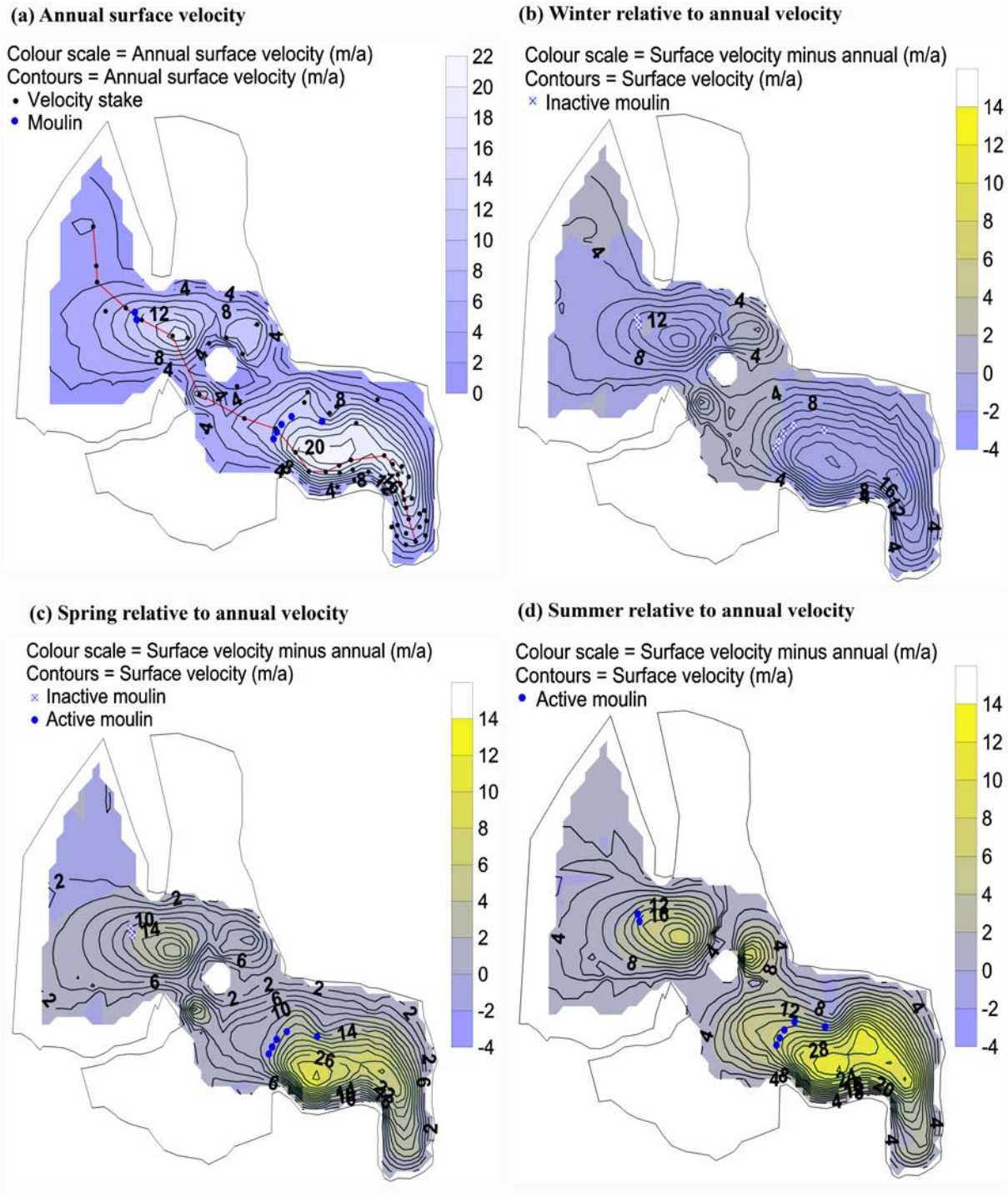
(a) Annual surface velocity
Colour scale = Annual surface velocity (m/a)
Contours = Annual surface velocity (m/a)
Velocity stake
Moulin
22
20
18
16
14
12
10
8
6
4
2
0
(b) Winter relative to annual velocity
Colour scale = Surface velocity minus annual (m/a)
Contours = Surface velocity (m/a)
Inactive moulin
14
12
10
8
6
4
2
0
-2
-4
(c) Spring relative to annual velocity
Colour scale = Surface velocity minus annual (m/a)
Contours = Surface velocity (m/a)
Inactive moulin
Active moulin
14
12
10
8
6
4
2
0
-2
-4
(d) Summer relative to annual velocity
Colour scale = Surface velocity minus annual (m/a)
Contours = Surface velocity (m/a)
Active moulin
14
12
10
8
6
4
2
0
-2
-4

Figure 2

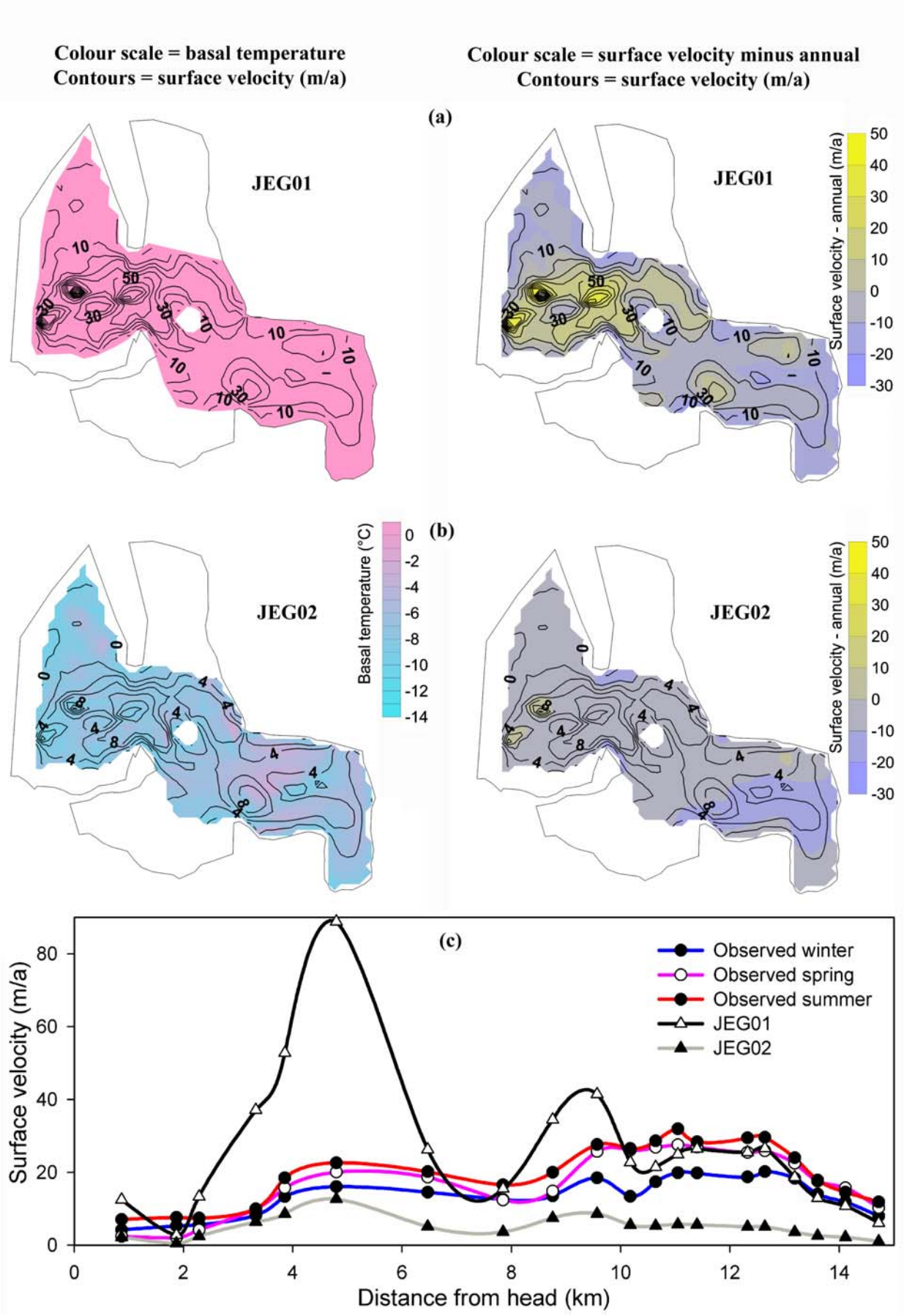
Colour scale = basal temperature
Contours = surface velocity (m/a)
Colour scale = surface velocity minus annual
Contours = surface velocity (m/a)
(a)
JEG01
JEG01
Surface velocity - annual (m/a)
50
40
30
20
10
0
-10
-20
-30
(b)
JEG02
JEG02
Basal temperature (°C)
0
-2
-4
-6
-8
-10
-12
-14
Surface velocity - annual (m/a)
(c)
Observed winter
Observed spring
Observed summer
JEG01
JEG02
Surface velocity (m/a)
Distance from head (km)

Figure 3

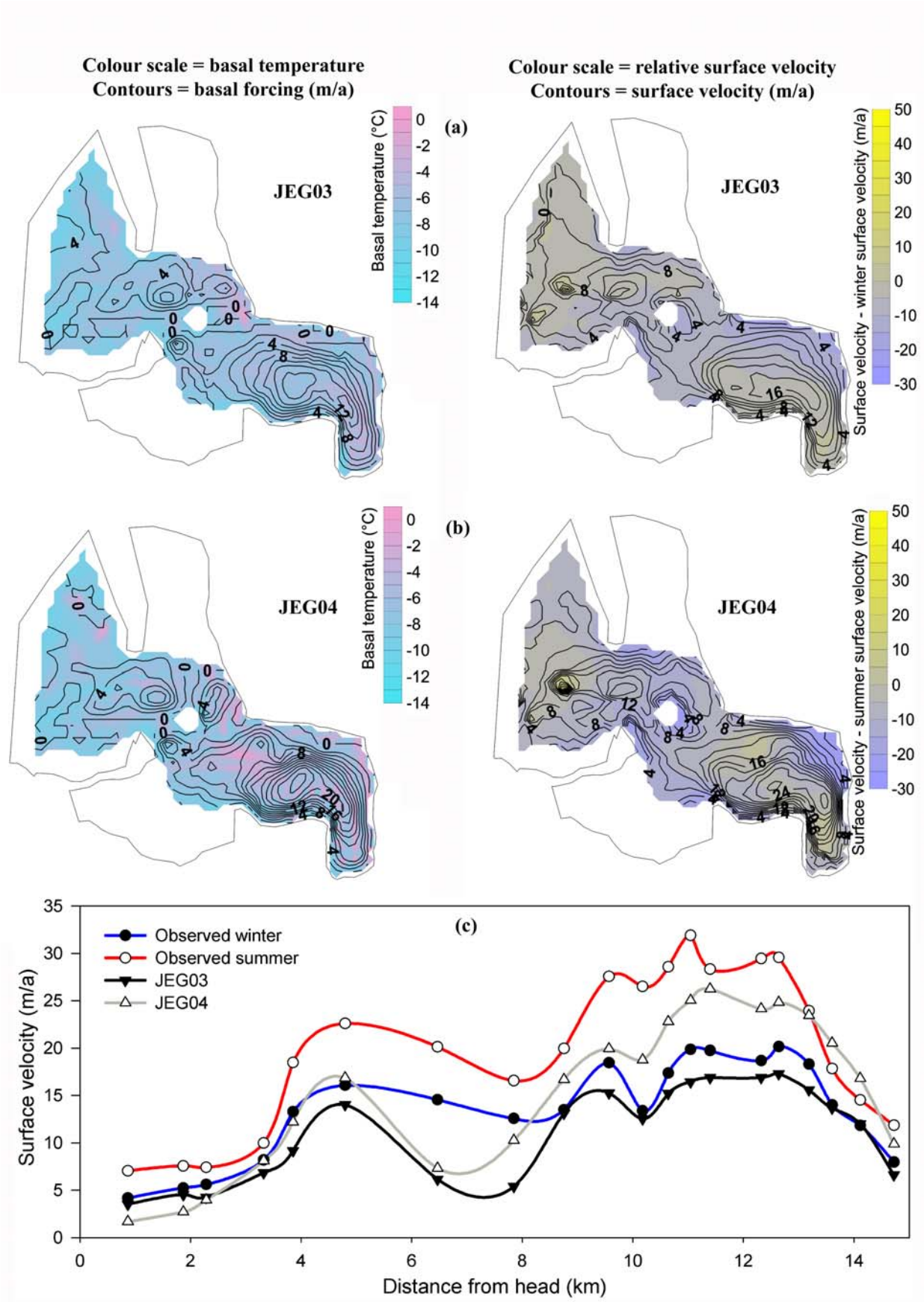
Colour scale = basal temperature
Contours = basal forcing (m/a)
Colour scale = relative surface velocity
Contours = surface velocity (m/a)
(a)
JEG03
Basal temperature (°C)
Surface velocity - winter surface velocity (m/a)
(b)
JEG04
Surface velocity - summer surface velocity (m/a)
(c)
Observed winter
Observed summer
JEG03
JEG04
Surface velocity (m/a)
Distance from head (km)

Figure 4

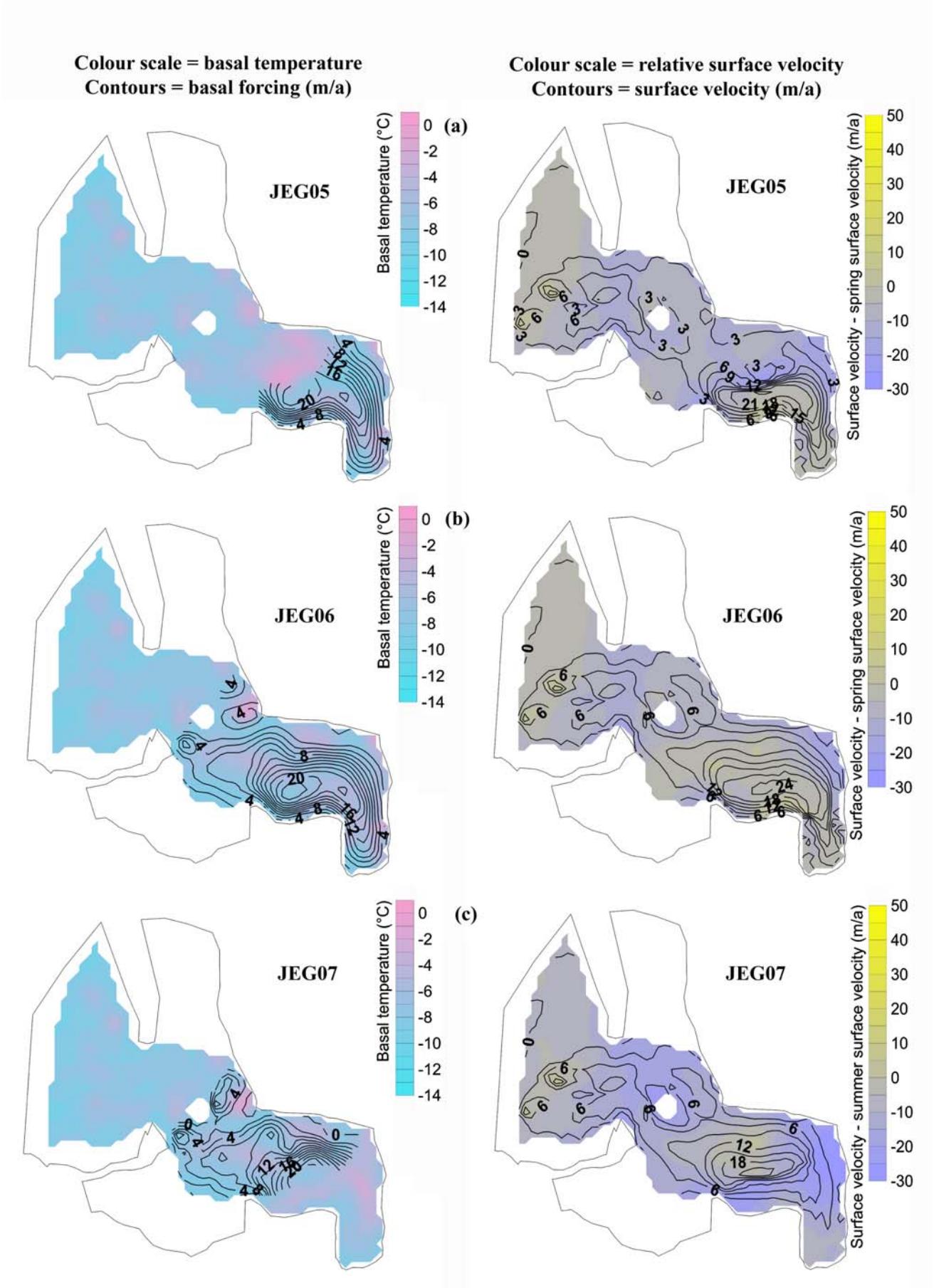


Figure 5 parts (a) to (c)

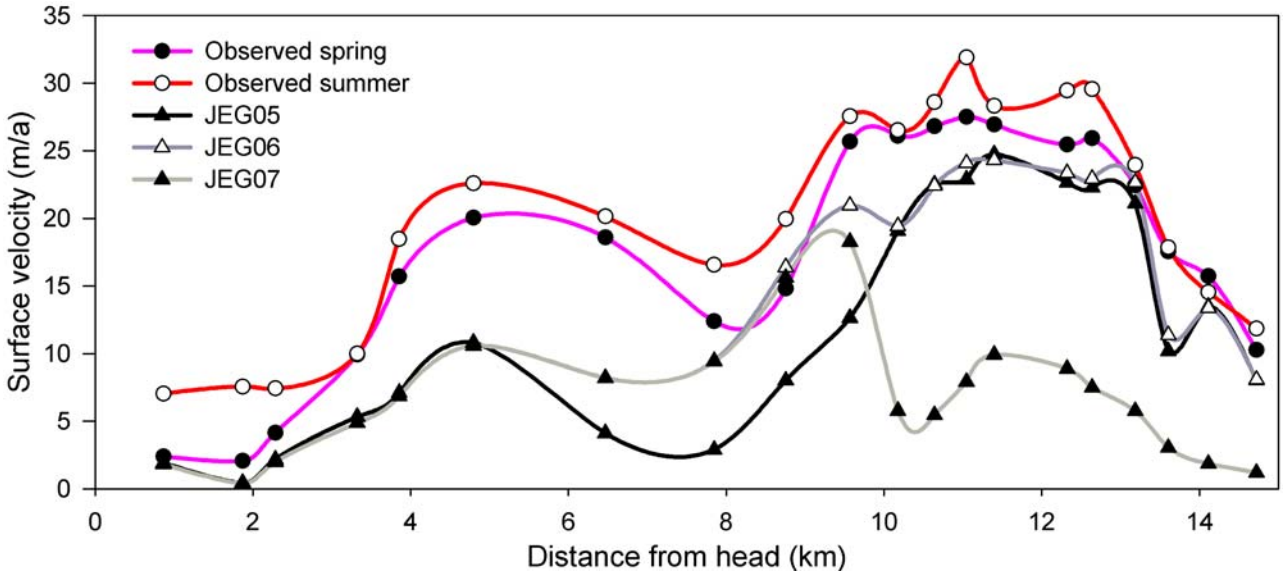


Figure 5 part (d)